



A Novel Fluorescent Aptasensor Based on Dual-labeled DNA Nanostructure for Simultaneous Detection of Ochratoxin A and Aflatoxin B1

Luyang Zhao¹ · Xiujun Liang¹ · Yong Liu² · Min Wei¹ · Huali Jin¹

Received: 22 June 2022 / Accepted: 2 November 2022 / Published online: 20 February 2023
© The Author(s), under exclusive licence to Springer Science+Business Media, LLC, part of Springer Nature 2023

Abstract

Based on DNA strand replacement reaction and aptamer-specific recognition, a simple dual-labeled DNA nanostructure is designed for the simultaneous detection of Ochratoxin A (OTA) and aflatoxin B1 (AFB₁). C1 is labeled with Cy3 and Cy5, while C2 and C3 are labeled with BHQ2. The fluorescence intensity of DNA nanostructure composed of C1, C2 and C3 is weak because of fluorescence resonance energy transfer. When OTA Aptamer (OTA-Apt) and AFB₁ Aptamer (AFB₁-Apt) are added to the homogeneous system at the same time, C1 can be replaced with the help of toehold strand displacement, resulting in fluorescence enhancement. In the presence of both OTA and AFB₁, the toehold strand displacement reaction is inhibited due to preferential binding between the target and their corresponding aptamers. The limit of detection of OTA was 0.007 ng/mL and that of AFB₁ was 0.03 ng/mL. The recoveries of OTA and AFB₁ were 96%–101% and 97%–101% in the corn sample, and 99%–101% and 92%–106% in the wine sample. Compared with other sensors, the preparation of this aptasensor needs simpler experimental steps and a shorter total-preparing time, confirming the convenient, rapid, and time-saving operation process.

Keywords Dual-labeled DNA nanostructure · DNA strand replacement reaction · Aptasensor · Simultaneous detection

Introduction

Ochratoxin A (OTA) and aflatoxin B1 (AFB₁) have strong hepatotoxicity, nephrotoxicity, immunotoxicity, and carcinogenic teratogenicity [1]. It has been reported that OTA and AFB₁ can coexist in wheat and maize [2, 3]. When OTA and AFB₁ coexist, toxins cause greater toxicity due to accumulation or synergy, and pose a greater threat to human health [4, 5]. Therefore, it is urgent to establish a rapid, safe, accurate, and simultaneous detection method of OTA and AFB₁ to accurately assess the degree of food pollution.

Traditional analysis methods include high-performance liquid chromatography (HPLC) [6] and high-performance liquid chromatography-tandem mass spectrometry (HPLC–MS) [7], but these methods are limited by expensive instruments, professionals and complex operating processes. The liquid crystal-based biosensor has also attracted wide attention due to its great potential in on-site detection, but its practical application is also limited because the liquid crystal is not resistant to high temperatures [8, 9]. At the same time, based on antibodies specific to mycotoxins, enzyme-linked immunosorbent assay [10] and immunochromatography [11] were developed for the simultaneous detection of various mycotoxins. However, mycotoxins are small molecules, so the production process of antibodies is complex and the stability is low, and it is difficult to produce high-quality antibodies, which seriously hinders the practicability of immunoassay in the detection of multiple mycotoxins. The aptamer is a single-stranded oligonucleotide sequence with high affinity and specificity for targets. As a new class of recognition elements, they not only have the same specific recognition ability as antibodies, but also have some other advantages such as easy synthesis, good chemical stability, good repeatability, easy storage and transportation [12, 13]. In addition, aptamers can easily modify functional groups,

✉ Min Wei
wei_min80@163.com

Huali Jin
jinhuali66@163.com

¹ College of Food Science and Technology, Henan Key Laboratory of Cereal and Oil Food Safety Inspection and Control, Henan University of Technology, Zhengzhou 450001, China

² College of Chemistry and Chemical Engineering, Henan University, Kaifeng 475004, China

fluorescent groups, biotins and enzymes, simplify the detection steps and make the sensor platform more flexible [14].

Due to the advantages of aptamer, it has been widely used in the fabrication of sensors. The colorimetric aptasensor is simple and intuitive, and has a good application in single target detection, but it has been greatly limited in the field of multivariate detection [15, 16]. Although the electrochemical aptasensor can be used for the detection of dual targets, the electrode surface modification is time-consuming and laborious, which significantly increases the preparation time of the aptasensor [17]. So far, fluorescent aptasensor has received extensive attention due to their simple operation, short analysis time, high sensitivity and good stability [18, 19].

Because of the easy modification, controllable self-assembly and good stability of DNA sequences, complex DNA nanostructures such as tweezers, walkers, gears and nanocages have been widely used in the biomolecular assembly, signal recognition and biosensors [20–22]. Although these complex nanostructures can be used to detect a variety of targets, the costs are prohibitive. Conversely, simple nanostructures can not only reduce the interference of other factors in the system, but also save costs.

In addition, enzyme-free DNA amplification technology has been widely concerned because of its low cost and high efficiency [23, 24]. In the enzyme-free amplification method, the strand displacement reaction refers to the displacement of one or more pre-hybridized strands, initiated by the toehold region and the single strand, and carried out by a rapid branch migration process [25]. The toehold region can first act as a recognition site to bind to a single strand, and then trigger a cascade of hybridization to form a partially or fully complementary DNA double strand [26]. This reaction allows for single-strand exponential amplification in less than 15 min without the presence of the enzyme [27], which provides an efficient way to control DNA hybridization and amplify target-binding signals. Thus, the strand displacement reaction is a very useful technique that provides straightforward solutions for the analysis of various objectives, such as nucleic acids and proteins. So far, the

combination of simple DNA nanostructures and DNA strand displacement techniques is rare in the detection of mycotoxins, especially in the simultaneous detection of multiple mycotoxins.

In this study, a fluorescent aptasensor based on DNA dual-labeled nanostructure was constructed using simple DNA nanostructures for simultaneous detection of OTA and AFB₁. In the beginning, C1 labeled by Cy3 and Cy5 can simultaneously hybridize with C2 labeled by BHQ2 (C2-BHQ2) and C3 labeled by BHQ2 (C3-BHQ2). And the fluorescence intensity of DNA nanostructure composed of C1, C2 and C3 is weak because of the fluorescence resonance energy transfer (FRET) between Cy3 and BHQ2, Cy5 and BHQ2. In the presence of OTA Aptamer (OTA-Apt) and AFB₁ Aptamer (AFB₁-Apt), OTA-Apt and AFB₁-Apt respectively combine with C2 and C3 by toehold-mediated chain replacement, so C1 labeled by Cy3 and Cy5 can be replaced, resulting in enhanced fluorescence intensity. In the presence of OTA and AFB₁, owing to the preferential binding between OTA and OTA-Apt, and the preferential binding between AFB₁ and AFB₁-Apt, toehold displacement reaction is inhibited. Then C1 labeled by Cy3 and Cy5 can combine with C2-BHQ2 and C3-BHQ2, then the fluorescence intensity has a significant decrease.

Experimental Section

Materials

All HPLC-purified DNA sequences were synthesized by Shanghai Sangon. The detailed sequences are provided in Table 1. Among them, M1 and N1 are part of C1, which are complementary to C2 and C3, respectively. AFB₁, OTA, zearalenone (ZEN) and deoxynivalenol (DON) were purchased from Sigma-Aldrich. Fumonisin B₁ (FB₁) was provided by Acros Organics. Wine and corn were obtained from a local supermarket in Zhengzhou, China. All the chemicals were of analytical grade and all aqueous solutions were prepared via ultra-pure water (18.25 MΩ).

Table 1 The DNA sequences used in this experiment

Oligonucleotides	Sequence (5'–3')
OTA-aptamer	GAT CGG GTG TGG GTG GCG TAA AGG GAG CAT CGG ACA
AFB ₁ -aptamer	TGC ACG TGT TGT CTC TCT GTG TCT CGT GC
C1	Cy5-AAT GGA TGT TGT CTC TCT GTC TTT TTT TTT TTT TTT TTT TTC AGA TAG TGT GGG TGG CGT AAA GGG A-Cy3
C2	BHQ2-TCC CTT TAC GCC ACC CAC ACC CGA TC
C3	GAC ACA GAG AGA CAA CAC GTG CA-BHQ2
M1	G TGT GGG TGG CGT AAA GGG A
N1	TGT TGT CTC TCT GT

Preparation of Dual-labeled DNA Nanostructure

Before the experiment, all containers were sterilized and the DNA was dissolved using 20 mM Tris buffer solution (20 mM Tris, 50 mM NaCl, 50 mM MgCl₂, pH 8.0). The dual-labeled DNA nanostructure was prepared based on the complementary pairing via the denaturation annealing process. Briefly, 10 μ L of C1, C2 and C3 at a concentration of 2 μ M were stirred in the PCR tube. The mixtures were put into a PCR instrument and heated to 95 °C for 10 min. Then, the DNA cooled to 4 °C at a rate of 1 °C/min. After 20 min at 4 °C, the dual-labeled DNA nanostructure was prepared.

Simultaneous Determination of OTA and AFB₁

The analytical methods of OTA and AFB₁ based on dual-labeled DNA nanostructure are as follows: 10 μ L of 2 μ M OTA-Apt and AFB₁-Apt, 10 μ L of OTA and AFB₁ at different concentrations were added to the prepared aptasensor, respectively. After that, the mixture was placed at 37 °C for 30 min and supplemented to 200 μ L with Tris–HCl solution. And the excitation scanning was measured by a Hitachi F-7100 fluorescence spectrophotometer. The slit width of excitation and emission were set at 5 nm, the voltage was set at 950 V, and the excitation wavelength was set at 530 nm (Cy3) and 635 nm (Cy5), respectively. The selectivity of the aptasensor to OTA and AFB₁ was evaluated by monitoring the relative fluorescent changes at 570 nm (Cy3) and 670 nm (Cy5) to 100 ng/mL other mycotoxins (FB₁, DON, ZEN) and their mixtures (OTA, AFB₁, FB₁, ZEN and DON). All experiments were measured at least three times.

OTA and AFB₁ Detection in Real Samples

The corn and wine were pretreated for OTA and AFB₁ detection in real samples [19]. Firstly, corn was ground into powder (1.0 g), and 1 mL of OTA and AFB₁ solution (OTA and AFB₁ concentrations were 10 ng/mL, 100 ng/mL and 1000 ng/mL, respectively) was added. After drying at room temperature, the extraction solvent (9 mL, methanol: water, 7:3 [v/v]) was added and stirred with vibration for 30 min. The actual concentrations of toxins in real samples at this time were 1 ng/mL, 10 ng/mL and 100 ng/mL. After that, the solutions were centrifuged at 5000 rpm for 10 min, and the supernatants were filtered by a 0.22 μ m filter, and then diluted to 100 mL with 20 mM Tris buffer. At this time, different concentrations of OTA and AFB₁ (0.1 ng/mL, 1 ng/mL, 10 ng/mL) in corn samples were obtained. Furthermore, 5.0 mL wine was mixed with different concentrations of OTA and AFB₁ (OTA and AFB₁ concentrations were 10 ng/mL, 100 ng/mL and 1000 ng/mL, respectively) solution and filtered with a 0.22 μ m filter membrane. Then the

solution was diluted to 100 mL with 20 mM Tris buffer. In the end, different concentrations of OTA and AFB₁ (0.1 ng/mL, 1 ng/mL, 10 ng/mL) were obtained from wine samples. The spiked samples can be used for real sample detection.

Results and Discussion

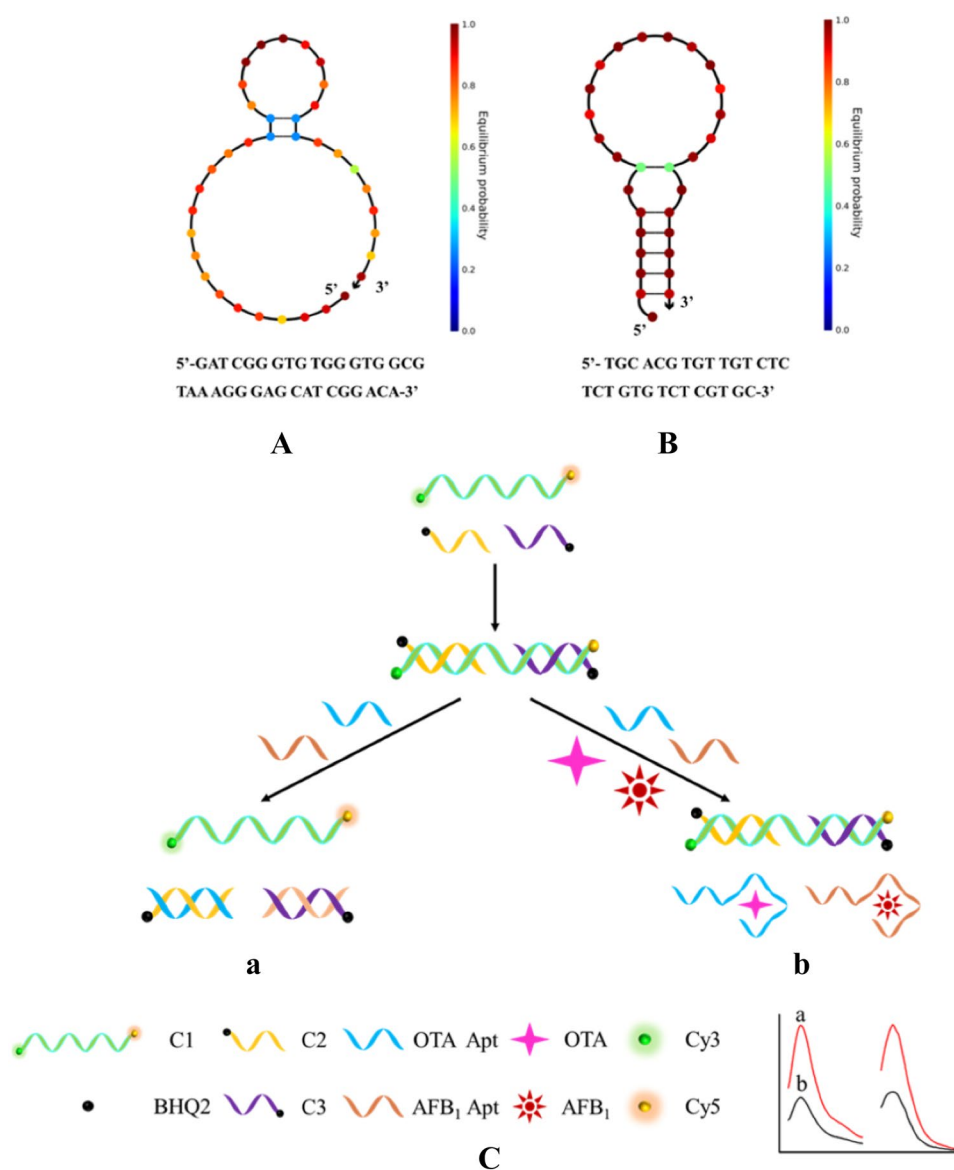
Design of the Fluorescent Aptasensor

The principle of the proposed fluorescent aptasensor was displayed in Scheme 1. C1 is labeled with Cy3 and Cy5, while C2 and C3 are labeled with BHQ2. When the self-assembly of the dual DNA labeled nanostructure is completed, the distance of Cy3 and BHQ2, Cy5 and BHQ2 are extremely close, resulting in the suppression of their fluorescence signal. When OTA-Apt and AFB₁-Apt are added to the homogeneous system, OTA-Apt and AFB₁-Apt can respectively combine with C2 and C3 by toehold-mediated chain replacement. At this time, Cy3 and Cy5 are far away from BHQ2, and the fluorescence signal is recovered. In the presence of OTA and AFB₁, OTA and AFB₁ preferentially combine with their respective aptamers to form complexes due to the affinity between the aptamer and the target. This phenomenon inhibits toehold-mediated chain replacement reaction. Then the C2 and C3 in the DNA dual-labeled nanostructure cannot be replaced, and the fluorescence signals of Cy3 and Cy5 are inhibited.

To simulate the reaction among DNA strands, the secondary structures of C1, C2, C3 OTA Apt and AFB₁ Apt at 37 °C were shown in Fig. 1A, which are predicted by the UNPACK online website (<http://www.nupack.org/>). The free energy and secondary structures of dual-strand DNA are also shown in Fig. 1B, C. Since the free energy of the dual-strand DNA formed by C1 and C2 ((a) in Fig. 1B), M1 and C2 ((b) in Fig. 1B) are higher than that of the dual-strand DNA formed by C2 and OTA-Apt ((c) in Fig. 1B), C2 will react with OTA-Apt preferentially, thus making C1 fall off. Similarly, because the free energy of C1 and C3 ((a) in Fig. 1C), N1 and C3 ((b) in Fig. 1C) forming dual chains are higher than that of C3 and AFB₁-Apt ((c) in Fig. 1C) forming double chains, C3 will preferentially react with AFB₁-Apt, resulting in C1 shedding. Therefore, theoretically speaking, the addition of OTA-Apt and AFB₁-Apt will cause C1 to be replaced, thus destroying the nanostructures formed by C1, C2 and C3.

To study the feasibility of this fluorescent aptasensor, the effect of OTA and AFB₁ on fluorescence intensity was investigated under optimized conditions. Figure 2A showed a high fluorescence intensity due to the weak FRET between BHQ2-Cy3/Cy5, with little change in fluorescence intensity at 570 nm and 670 nm with the addition of target-free buffer solution. In the presence of OTA, the fluorescence intensity

Scheme 1 Schematic illustration of the formation of fluorescent aptasensor based on dual-labeled DNA nanostructure. The two-dimensional structure of OTA aptamer (**A**) and AFB₁ aptamer (**B**) at 37 °C were predicted by NUPACK. (**C**) The working principle of the fluorescent aptasensor for the simultaneous detection of OTA and AFB₁ was based on a dual-labeled DNA nanostructure



was decreased by 57% at 570 nm and remained unchanged at 670 nm (Fig. 2B). Similarly, in the presence of AFB₁, the fluorescence intensity was reduced by half at 670 nm and remained constant at 570 nm (Fig. 2C). When OTA and AFB₁ were present simultaneously, the fluorescence intensity of the aptasensor decreased significantly at 570 nm and 670 nm due to the separation of aptamer from DNA nanostructure by target (Fig. 2D). The above results indicated that the fluorescent aptasensor can be used for the simultaneous detection of OTA and AFB₁.

The construction of the aptasensor was characterized by 3.5% agarose gel electrophoresis. As shown in Fig. 3A, all DNA nanostructures and strands can be displayed in the corresponding lanes. The assembled dual-labeled DNA nanostructure showed the lowest migration in lane 1, demonstrating the successful formation of the aptasensor. Owing to 67

bases, C1 showed the slower move in lane 2. Since C2 and C3 were short chains with only 26 and 23 bases, respectively, the migration rate was fast and ran at the front end. At the same time, because they were single chains and have few bases, there were few dyes bound and only weak light. The above gel electrophoresis results indicated that the self-assembly of dual-labeled DNA nanostructure was successful.

In Fig. 3B, lane 1 represents the dual-labeled DNA nanostructure. In the presence of OTA-aptamer and AFB₁-aptamer, the gel electrophoresis result was shown in lane 2 of Fig. 3B. At this time, there are still a few dual-labeled DNA nanostructure in the system, so the migration rate of the first band is the same as that of lane 1. However, the second band in lane 2 was relatively fast than lane 1, which was due to the fact that OTA aptamer and AFB₁ aptamer

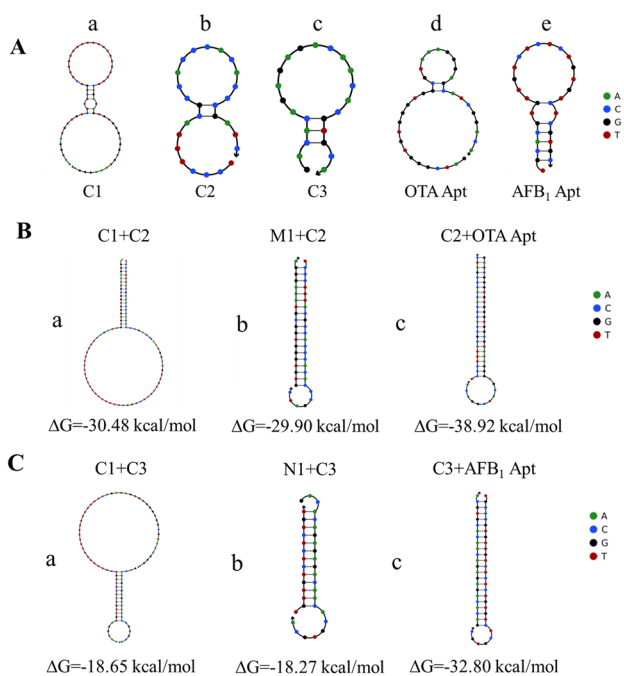
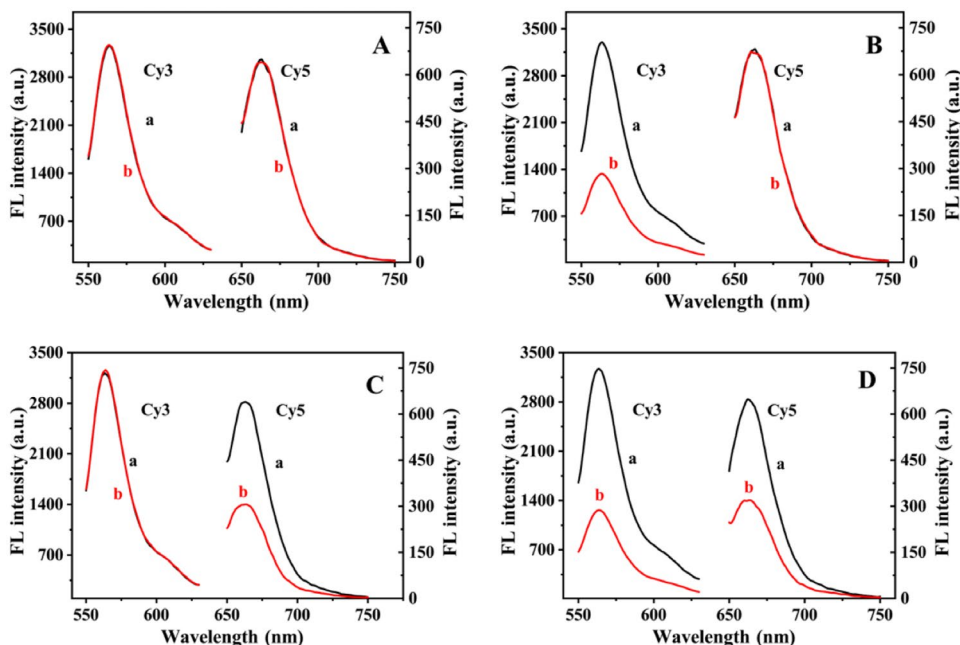


Fig. 1 **A** The secondary structures of **a** C1, **b** C2, **c** C3, **d** OTA-Apt and **e** AFB₁-Apt at 37°C; **B** the free energy and secondary structures for formed double strands of **a** C1+C2, **b** M1+C2, **c** OTA-Apt+C2 at 37°C; **C** the free energy and secondary structures for formed double strands of **a** C1+C3, **b** N1+C3, **c** AFB₁-Apt+C3 at 37°C

form double chains with C2 and C3, respectively. Lane 3 represents the result when OTA and AFB₁ are present at the same time, the first band of lane 3 migrated at the same rate as lane 1. This is because OTA and AFB₁ form complexes with aptamers respectively, resulting in the presence of a

Fig. 2 Representative fluorescence spectra of aptasensor system without target (**A**); only OTA (**B**); only AFB₁ (**C**); OTA and AFB₁ both present (**D**). The fluorescence spectra of aptasensor before (**a**) and after (**b**) target addition [$C_{OTA} = C_{AFB1} = 5 \text{ ng/mL}$]



large number of double-labeled DNA nanostructures in the system.

In conclusion, the above electrophoresis results indicated that the aptasensor was successfully prepared and can be successfully used for OTA and AFB₁ detection.

Optimization of Detection Conditions

As shown in Fig. 4, the incubation time for C1, C2, and C3 and the reaction time of OTA and AFB₁ were optimized. With the increase of incubation time for C1, C2 and C3, the quenching effect of BHQ2 on Cy3 and Cy5 on C1 increased, and the fluorescence signal gradually decreased. When the incubation time reached 80 min, it no longer decreases, so 80 min was optimal at this time. With the increase in reaction time, the fluorescent intensity gradually increased and then became stabilized. When the reaction time reached 30 min, the maximum change indicated the optimal reaction time.

Simultaneous detection of OTA and AFB₁ using fluorescent aptasensors

As depicted in Fig. 5A, the fluorescence intensity at 570 nm decreased with increasing concentrations of OTA in the range of 0.01 to 500 ng/mL. The logarithm of OTA concentration displayed an excellent linear relationship with $F_0 - F$ (F_0 and F are the emission intensities of Cy3 in the absence and presence of OTA) (Fig. 5B). The corresponding linear equation was calculated to be $y = 645.3x + 1516$, with a correlation coefficient of $R^2 = 0.998$ in the range of 0.01 to 100 ng/mL. The LOD of OTA was calculated to be

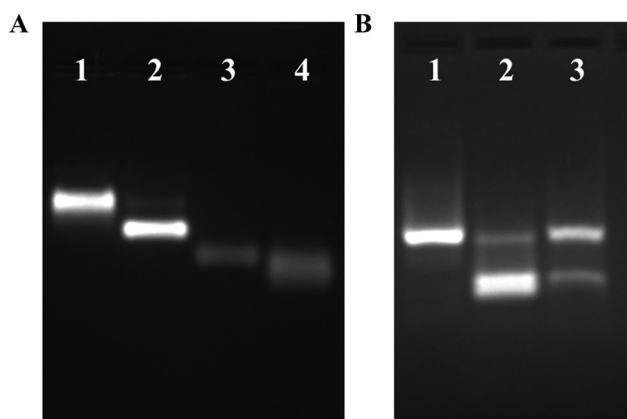


Fig. 3 The agarose gel electrophoresis characterization of **A** C1+C2+C3 (lane 1), C1 (lane 2), C2 (lane 3), C3 (lane 4) and **B** C1+C2+C3 (lane 1), C1+C2+C3+OTA aptamer+AFB₁ aptamer (lane 2), C1+C2+C3+OTA aptamer+AFB₁ aptamer+OTA+AFB₁ (lane 3); the concentrations of all ssDNA were 10 μ M

0.007 ng/mL. In addition, the presence of AFB₁ reduced the fluorescence intensity at 670 nm (Fig. 5C). In the range of 0.1–100 ng/mL, F_0/F increased with the increase of AFB₁ concentration, and the linear equation was $y = 146.3x + 261$, $R^2 = 0.996$ (Fig. 5D). The LOD was 0.03 ng/mL ($S/N = 3$). To further highlight the performance of the fluorescence aptasensor, Table 2 summarizes the comparison of different

analytical methods for the detection of OTA and AFB₁. The proposed fluorescence aptasensor can realize the simultaneous detection of OTA and AFB₁, and has a wider detection range and lower LOD compared with other analytical methods. Also, as compared with other aptasensors, the experimental steps are simpler and the total preparing time is shorter, confirming the convenient, rapid and time-saving operation process.

Furthermore, the selectivity of the aptasensor was evaluated by comparing the fluorescence changes of different mycotoxins under the same conditions. Figure 6 showed that the F_0/F significantly increased in the existence of OTA, AFB₁ and the corresponding mixtures. However, the F_0/F changed little when the interfering mycotoxins including FB₁, ZEN and DON existed. Moreover, the F_0/F between the target and the mixture was similar, indicating that there was no interaction between OTA and AFB₁. This was mainly ascribed to the high affinity between the aptamer and its target. These results demonstrate that the fluorescent aptasensor has a broad application prospect in the simultaneous detection of OTA and AFB₁ in food.

Practical detections for OTA and AFB₁

In practical applications, this fluorescent aptasensor was applied to determine the concentrations of OTA and AFB₁

Fig. 4 The fluorescent intensity of Cy3 (A) and Cy5 (B) at different incubation times for C1, C2, and C3; (C) the fluorescent intensity after adding OTA at different reaction times (10 min, 20 min, 30 min, 40 min, 50 min); (D) the fluorescent intensity after adding AFB₁ at different reaction time (10 min, 20 min, 30 min, 40 min, 50 min) [$C_{OTA} = C_{AFB_1} = 5$ ng/mL] ($n = 3$)

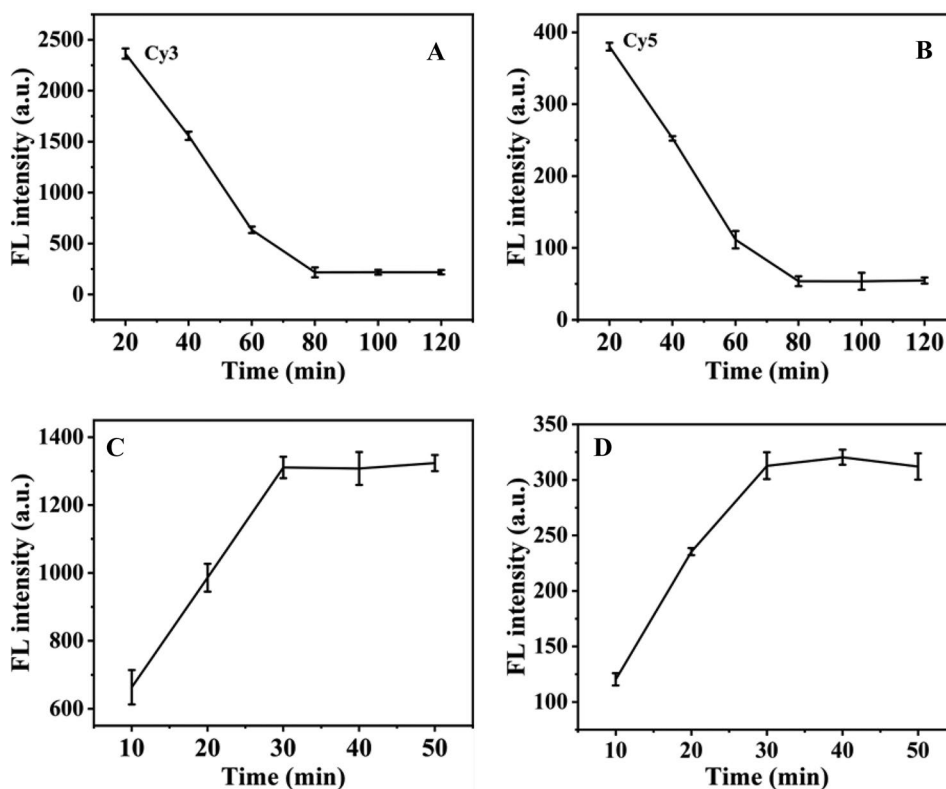
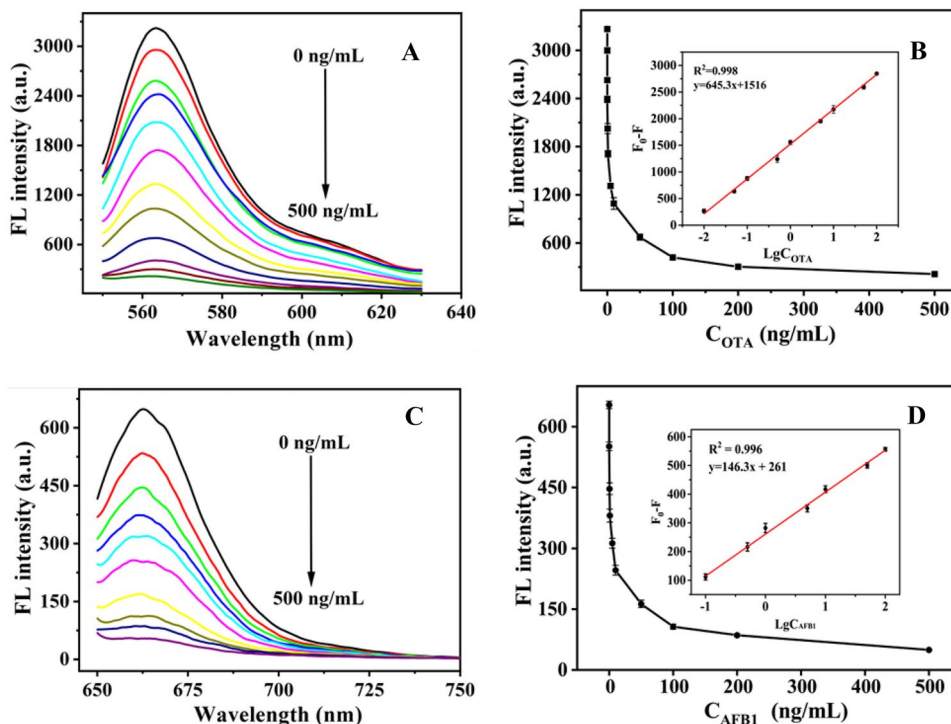


Fig. 5 Representative fluorescence emission spectra of aptasensor at different concentrations of OTA (0.01–500 ng/mL) (A) and AFB₁ (0.1–500 ng/mL) (C). The corresponding calibration plot of relative fluorescence intensity toward OTA (B) and AFB₁ (D) concentrations (n=3). Inset: The linear relationship of relative fluorescence intensity toward the logarithm of OTA and AFB₁ concentration



in corn and wine samples. The recoveries of OTA and AFB₁ in the corn sample ranged from 96 to 101% and 97% to 101% respectively, and those in the wine sample were 99% to 101% and 92% to 106% (Table 3). All of these results

indicated that the fluorescent aptasensor detection system has obvious advantages over other methods, which can be used as an alternative method for the practical application of OTA and AFB₁.

Table 2 The comparison with other analytical methods for OTA and AFB₁ detection

Mycotoxins	Method	Step required ^a	Sensors preparing time ^b	Detection range (ng/mL)	LOD (ng/mL)	Ref
OTA	Electrochemistry	3	> 5 h	0.08–200	0.03	[28]
	Electrochemistry	3	4.5 h	0.78–8.74	0.07	[29]
	Immunoassay	4	8.5 h	0.0125–8	0.01	[30]
	Colorimetric	2	> 4 h	0.01–10	0.008	[31]
	Colorimetric	4	> 24 h	0.1–10	0.08	[32]
	Fluorescence	3	4 h	0.10–10	0.015	[33]
	Fluorescence	2	> 4 h	0.40–20	0.08	[34]
	Fluorescence	2	2 h	0.01–100	0.007	This work
AFB ₁	Electrochemistry	3	> 3 h	0.25–16	0.25	[35]
	Electrochemistry	4	> 6 h	0.05–6	0.05	[36]
	Immunoassay	3	3.5 h	1–30	0.62	[37]
	Colorimetric	2	> 5 h	1–6	0.18	[38]
	Fluorescence	3	> 5 h	0.1–0.8	0.07	[39]
	Fluorescence	3	5 h	0.1–10	0.02	[40]
	Fluorescence	2	2 h	0.1–100	0.03	This work

^{a, b}The steps and time were estimated from the description of an operational process

Fig. 6 Selectivity analysis of the fluorescent aptasensors for OTA (A) and AFB₁ (B) (n=3). The Mix contains OTA, AFB₁, FB₁, ZEN and DON [$C_{OTA} = C_{AFB_1} = 5$ ng/mL; $C_{FB_1} = C_{ZEN} = C_{DON} = 100$ ng/mL]

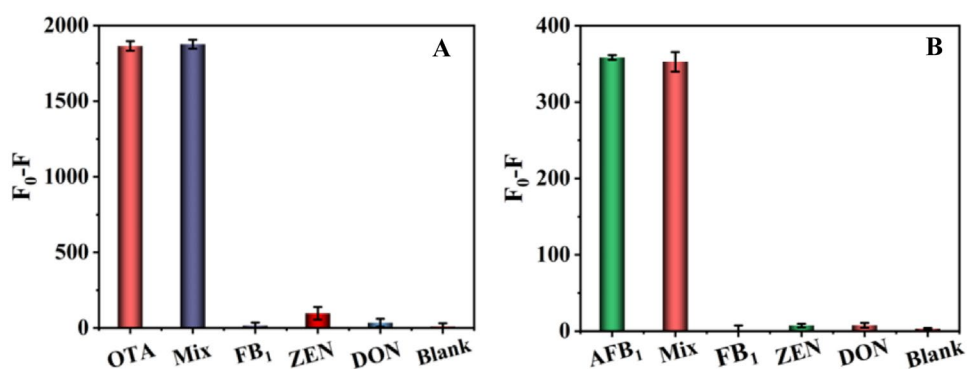


Table 3 Test results of OTA and AFB₁ spiked samples (n=3)

Sample	Mycotoxins	Spiked amount (ng/mL)	Found amount (ng/mL)	Recovery (%)	RSD (%)
Corn	OTA	0	ND	-	-
		0.1	0.101	101	8.3
		1	0.96	96	3.8
		10	10.13	101	4.7
	AFB ₁	0	ND	-	-
		0.1	0.101	101	7.0
		1	0.97	97	6.1
Wine	OTA	0	ND	-	-
		0.1	0.099	99	9.7
		1	1.01	101	4.4
		10	10.0	100	8.1
	AFB ₁	0	ND	-	-
		0.1	0.098	98	4.2
		1	1.06	106	3.1
		10	9.20	92	1.3

ND Not detected

Conclusions

In summary, a fluorescent aptasensor based on the dual-labeled DNA nanostructure was successfully developed for the simultaneous detection of OTA and AFB₁. The stable dual-labeled DNA nanostructure is assembled from C1, C2 and C3, which can realize the detection of OTA and AFB₁ by comparing the fluorescence changes before and after the addition of the targets. In addition, with the help of toehold strand displacement, the fluorescence resonance energy transfer is effectively blocked, resulting in a change in the fluorescence signal. Moreover, due to the high selectivity of the OTA and AFB₁ aptamers, the aptasensor presents an excellent specificity. The aptasensor can also be applied to the analysis of OTA and AFB₁ in the complicated matrix (corn and wine samples). For the preparation of the aptasensor, the experimental steps are

simpler and the total preparation time is shorter, confirming the convenient, rapid and time-saving operation process. In conclusion, the rational design of this fluorescent aptasensor provides a promising method for the simultaneous detection of multiple mycotoxins and promotes the application of aptamer in sensors.

Supplementary Information The online version contains supplementary material available at <https://doi.org/10.1007/s10895-022-03071-5>.

Author's contributions Luyang Zhao: Investigation, Methodology, Validation and Writing-Original Draft. Xiujun Liang: Validation and Writing-Original Draft. Yong Liu: Supervision, Resources. Min Wei: Conceptualization, Methodology, Resources, Supervision and Funding acquisition. Huali Jin: Methodology, Resources, Supervision.

Funding This study was funded by the Key Scientific and Technological Project of Henan Province (212102310001), the Special Project for Collaborative Innovation of Zhengzhou (21ZZXTCX15), and the Innovative Funds Plan of Henan University of Technology (2021ZKCJ13).

Data Availability The datasets generated during and/or analysed during the current study are available from the corresponding author on reasonable request.

Declarations

Competing interests The authors declare no competing interests.

Ethics approval Not applicable.

Consent to participate Not applicable.

Consent for publication Not applicable.

Conflict of interest The authors have no relevant financial or non-financial interests to disclose.

References

- Sun S, Zhao R, Xie Y, Liu Y (2019) Photocatalytic degradation of aflatoxin B₁ by activated carbon supported TiO₂ catalyst. *Food Control* 100:183–188. <https://doi.org/10.1016/j.foodcont.2019.01.014>
- Tittlemier SA, Cramer B, Dall'Asta C, Iha MH, Lattanzio VMT, Malone RJ, Maragos C, Solfrizzo M, Stranska-Zachariasova M, Stroka J (2019) Developments in mycotoxin analysis: an update for 2017–2018. *World Mycotoxin J* 12(1):3–29. <https://doi.org/10.3920/wmj2018.2398>
- Kolpin DW, Schenzel J, Meyer MT, Phillips PJ, Hubbard LE, Scott T-M, Bucheli TD (2014) Mycotoxins: Diffuse and point source contributions of natural contaminants of emerging concern to streams. *Sci Total Environ* 470:669–676. <https://doi.org/10.1016/j.scitotenv.2013.09.062>
- Van Pamel E, Verbeken A, Vlaemynck G, De Boever J, Daeseleire E (2011) Ultrahigh-Performance Liquid Chromatographic-Tandem Mass Spectrometric Multimycotoxin Method for Quantitating 26 Mycotoxins in Maize Silage. *J Agric Food Chem* 59(18):9747–9755. <https://doi.org/10.1021/jf202614h>
- Sun S, Zhao R, Xie Y, Liu Y (2021) Reduction of aflatoxin B₁ by magnetic graphene oxide/TiO₂ nanocomposite and its effect on quality of corn oil. *Food Chem*. <https://doi.org/10.1016/j.foodchem.2020.128521>
- Liu C, Cao Y, Zhao T, Wang X, Fang G, Wang S (2021) A Novel Multi-purpose MIP for SPE-HPLC and QCM Detection of Carbaryl Residues in Foods. *Food Anal Methods* 14(2):331–343. <https://doi.org/10.1007/s12161-020-01875-4>
- Xue X, Selvaraj JN, Zhao L, Dong H, Liu F, Liu Y, Li Y (2014) Simultaneous Determination of Aflatoxins and Ochratoxin A in Bee Pollen by Low-Temperature Fat Precipitation and Immunoaffinity Column Cleanup Coupled with LC-MS/MS. *Food Anal Methods* 7(3):690–696. <https://doi.org/10.1007/s12161-013-9723-4>
- Khoshbin Z, Abnous K, Taghdisi SM, Verdian A, Sameiyan E, Ramezani M, Alibolandi M (2022) An ultra-sensitive dual-responsive aptasensor with combination of liquid crystal and intercalating dye molecules: A food toxin case study. *Food Chem*. <https://doi.org/10.1016/j.foodchem.2022.132265>
- Khoshbin Z, Abnous K, Taghdisi SM, Verdian A (2021) Liquid crystal-based biosensors as lab-on-chip tools: Promising for future on-site detection test kits. *TrAC, Trends Anal Chem* 142. <https://doi.org/10.1016/j.trac.2021.116325>
- Zhao F, Tian Y, Shen Q, Liu R, Shi R, Wang H, Yang Z (2019) A novel nanobody and mimotope based immunoassay for rapid analysis of aflatoxin B₁. *Talanta* 195:55–61. <https://doi.org/10.1016/j.talanta.2018.11.013>
- Wang Y-K, Yan Y-X, Li S-Q, Wang H-a, Ji W-H, Sun J-H (2013) Simultaneous Quantitative Determination of Multiple Mycotoxins in Cereal and Feedstuff Samples by a Suspension Array Immunoassay. *J Agric Food Chem* 61(46):10948–10953. <https://doi.org/10.1021/jf4036029>
- Seok Y, Byun J-Y, Shim W-B, Kim M-G (2015) A structure-switchable aptasensor for aflatoxin B₁ detection based on assembly of an aptamer/split DNAzyme. *Anal Chim Acta* 886:182–187. <https://doi.org/10.1016/j.aca.2015.05.041>
- Zhu C, Liu D, Li Y, Shen X, Ma S, Liu Y, You T (2020) Ratiometric electrochemical aptasensor for ultrasensitive detection of Ochratoxin A based on a dual signal amplification strategy: Engineering the binding of methylene blue to DNA. *Biosens Bioelectron*. <https://doi.org/10.1016/j.bios.2019.111814>
- Iliuk AB, Hu L, Tao WA (2011) Aptamer in Bioanalytical Applications. *Anal Chem* 83(12):4440–4452. <https://doi.org/10.1021/ac201057w>
- Yang C, Wang Y, Marty J-L, Yang X (2011) Aptamer-based colorimetric biosensing of Ochratoxin A using unmodified gold nanoparticles indicator. *Biosens Bioelectron* 26(5):2724–2727. <https://doi.org/10.1016/j.bios.2010.09.032>
- Khoshbin Z, Moeenfarid M, Abnous K, Taghdisi SM (2023) Nanogold mediated aptasensor for colorimetric monitoring of acrylamide: Smartphone readout strategy for on-site food control. *Food Chem*. <https://doi.org/10.1016/j.foodchem.2022.133983>
- Wei M, Xin L, Feng S, Liu Y (2020) Simultaneous electrochemical determination of ochratoxin A and fumonisin B₁ with an aptasensor based on the use of a Y-shaped DNA structure on gold nanorods. *Microchim Acta* 187(2). <https://doi.org/10.1007/s00604-019-4089-y>
- Ren W, Pang J, Ma R, Liang X, Wei M, Suo Z, He B, Liu Y (2022) A signal on-off fluorescence sensor based on the self-assembly DNA tetrahedron for simultaneous detection of ochratoxin A and aflatoxin B₁. *Anal Chim Acta*. <https://doi.org/10.1016/j.aca.2022.339566>
- Suo Z, Liang X, Jin H, He B, Wei M (2021) A signal-enhancement fluorescent aptasensor based on the stable dual cross DNA nanostructure for simultaneous detection of OTA and AFB₁. *Anal Bioanal Chem* 413(30):7587–7595. <https://doi.org/10.1007/s00216-021-03723-8>
- Huang R, He N, Li Z (2018) Recent progresses in DNA nanostructure-based biosensors for detection of tumor markers. *Biosens Bioelectron* 109:27–34. <https://doi.org/10.1016/j.bios.2018.02.053>
- Gong X, Zhou W, Li D, Chai Y, Xiang Y, Yuan R (2015) RNA-regulated molecular tweezers for sensitive fluorescent detection of microRNA from cancer cells. *Biosens Bioelectron* 71:98–102. <https://doi.org/10.1016/j.bios.2015.04.003>
- Xiong Z, Wang Q, Xie Y, Li N, Yun W, Yang L (2021) Simultaneous detection of aflatoxin B₁ and ochratoxin A in food samples by dual DNA tweezers nanomachine. *Food Chem*. <https://doi.org/10.1016/j.foodchem.2020.128122>
- Han B, Fang C, Sha L, Jalalah M, Al-Assiri MS, Harraz FA, Cao Y (2021) Cascade strand displacement reaction-assisted aptamer-based highly sensitive detection of ochratoxin A. *Food Chem*. <https://doi.org/10.1016/j.foodchem.2020.127827>
- Park Y, Lee CY, Kang S, Kim H, Park KS, Park HG (2018) Universal, colorimetric microRNA detection strategy based on target-catalyzed toehold-mediated strand displacement reaction. *Nanotechnology* 29(8). <https://doi.org/10.1088/1361-6528/aaa3a3>
- Song X, Ding Q, Pu Y, Zhang J, Sun R, Yin L, Wei W, Liu S (2021) Application of the Dimeric G-Quadruplex and toehold-mediated strand displacement reaction for fluorescence biosensing of ochratoxin A. *Biosens Bioelectron*. <https://doi.org/10.1016/j.bios.2021.113537>
- Yin J, Liu Y, Wang S, Deng J, Lin X, Gao J (2018) Engineering a universal and label-free evaluation method for mycotoxins

- detection based on strand displacement amplification and G-quadruplex signal amplification. *Sens Actuators B* 256:573–579. <https://doi.org/10.1016/j.snb.2017.10.083>
27. Bader A, Cockroft SL (2020) Conformational enhancement of fidelity in toehold-sequestered DNA nanodevices. *Chem Commun* 56(38):5135–5138. <https://doi.org/10.1039/d0cc00882f>
 28. Zhu X, Kou F, Xu H, Han Y, Yang G, Huang X, Chen W, Chi Y, Lin Z (2018) Label-free ochratoxin A electrochemical aptasensor based on target-induced noncovalent assembly of peroxidase-like graphitic carbon nitride nanosheet. *Sens Actuators B* 270:263–269. <https://doi.org/10.1016/j.snb.2018.05.048>
 29. Bonel L, Vidal JC, Duato P, Castillo JR (2011) An electrochemical competitive biosensor for ochratoxin A based on a DNA biotinylated aptamer. *Biosens Bioelectron* 26(7):3254–3259. <https://doi.org/10.1016/j.bios.2010.12.036>
 30. Wang Y, Hu X, Pei Y, Sun Y, Wang F, Song C, Yin M, Deng R, Li Z, Zhang G (2015) Selection of phage-displayed minotopes of ochratoxin A and its detection in cereal by ELISA. *Anal Methods* 7(5):1849–1854. <https://doi.org/10.1039/c4ay02290d>
 31. Lai W, Guo J, Wu Q, Chen Y, Cai Q, Wu L, Wang S, Song J, Tang D (2020) A novel colorimetric immunoassay based on enzyme-regulated instant generation of Turnbull's blue for the sensitive determination of ochratoxin A. *Analyst* 145(6):2420–2424. <https://doi.org/10.1039/c9an02447f>
 32. Huang L, Chen K, Zhang W, Zhu W, Liu X, Wang J, Wang R, Hu N, Suo Y, Wang J (2018) ssDNA-tailorable oxidase-mimicking activity of spinel MnCo₂O₄ for sensitive biomolecular detection in food sample. *Sens Actuators B* 269:79–87. <https://doi.org/10.1016/j.snb.2018.04.150>
 33. Liu R, Li W, Cai T, Deng Y, Ding Z, Liu Y, Zhu X, Wang X, Liu J, Liang B, Zheng T, Li J (2018) TiO₂ Nanolayer-Enhanced Fluorescence for Simultaneous Multiplex Mycotoxin Detection by Aptamer Microarrays on a Porous Silicon Surface. *ACS Appl Mater Interfaces* 10(17):14447–14453. <https://doi.org/10.1021/acsami.8b01431>
 34. Wu K, Ma C, Zhao H, Chen M, Deng Z (2019) Sensitive aptamer-based fluorescence assay for ochratoxin A based on RNase H signal amplification. *Food Chem* 277:273–278. <https://doi.org/10.1016/j.foodchem.2018.10.130>
 35. Goud KY, Catanante G, Hayat A, Satyanarayana M, Gobi KV, Marty JL (2016) Disposable and portable electrochemical aptasensor for label free detection of aflatoxin B1 in alcoholic beverages. *Sens Actuators B* 235:466–473. <https://doi.org/10.1016/j.snb.2016.05.112>
 36. Goud KY, Hayat A, Catanante G, Satyanarayana M, Gobi KV, Marty JL (2017) An electrochemical aptasensor based on functionalized graphene oxide assisted electrocatalytic signal amplification of methylene blue for aflatoxin B1 detection. *Electrochim Acta* 244:96–103. <https://doi.org/10.1016/j.electacta.2017.05.089>
 37. Migliorini FL, dos Santos DM, Soares AC, Mattoso LHC, Oliveira Jr ON, Correa DS (2020) Design of a low-cost and disposable paper-based immunosensor for the rapid and sensitive detection of aflatoxin B1. *Chemosensors* 8(3). <https://doi.org/10.3390/chemosensors8030087>
 38. Lerd Sri J, Chananchana W, Upan J, Sridara T, Jakmune J (2020) Label-free colorimetric aptasensor for rapid detection of aflatoxin B1 by utilizing cationic perylene probe and localized surface plasmon resonance of gold nanoparticles. *Sens Actuators B*. <https://doi.org/10.1016/j.snb.2020.128356>
 39. Guo M, Hou Q, Waterhouse GIN, Hou J, Ai S, Li X (2019) A simple aptamer-based fluorescent aflatoxin B1 sensor using humic acid as quencher. *Talanta*. <https://doi.org/10.1016/j.talanta.2019.120131>
 40. Wei M, Zhao F, Xie Y (2020) A novel gold nanostars-based fluorescent aptasensor for aflatoxin B1 detection. *Talanta*. <https://doi.org/10.1016/j.talanta.2019.120599>

Publisher's Note Springer Nature remains neutral with regard to jurisdictional claims in published maps and institutional affiliations.

Springer Nature or its licensor (e.g. a society or other partner) holds exclusive rights to this article under a publishing agreement with the author(s) or other rightsholder(s); author self-archiving of the accepted manuscript version of this article is solely governed by the terms of such publishing agreement and applicable law.